Laser-driven multi-MeV high-purity proton acceleration via anisotropic ambipolar expansion of micron-scale hydrogen clusters

Satoshi Jinno
Japan Atomic Energy Agency
Masato Kanasaki
Kobe University
Takafumi Asai
Kobe University
Ryutaro Matsui
Kyoto University
Alexander Pirozhkov
National Institutes for Quantum and Radiological Science and Technology
Koichi Ogura
National Institutes for Quantum and Radiological Science and Technology
Akito Sagisaka
National Institutes for Quantum and Radiological Science and Technology
Yasuhiro Miyasaka
National Institutes for Quantum Science and Technology (QST)
Nobuhiko Nakanii
National Institutes for Quantum Science and Technology (QST)
Masaki Kando
National Institutes for Quantum and Radiological Science and Technology
Nobuko Kitagawa
Nagoya University
Kunihiro Morishima
Nagoya University
Satoshi Kodaira
National Institutes for Quantum Science and Technology (QST)
Yasuaki Kishimoto
Kyoto University
Tomoya Yamauchi
Kobe-University
Mitsuru Uesaka

The University of Tokyo
Hiromitsu Kiriyama
QST/KPSI
Yuji Fukuda (fukuda.yuji@qst.go.jp)
National Institutes for Quantum Science and Technology (QST) https://orcid.org/0000-0002-1348-0483

Article

Keywords:

Posted Date: February 8th, 2022

DOI: https://doi.org/10.21203/rs.3.rs-1338789/v1

Laser-driven multi-MeV high-purity proton acceleration via anisotropic ambipolar expansion of micron-scale hydrogen clusters

S. Jinno,[1, a)] M. Kanasaki,[2] T. Asai,[2, 3] R. Matsui,[4] A. S. Pirozhkov,[3] K. Ogura,[3] A. Sagisaka,[3] Y. Miyasaka,[3] N. Nakanii,[3] M. Kando,[3] N. Kitagawa,[5] K. Morishima,[5] S. Kodaira,[6] Y. Kishimoto,[4] T. Yamauchi,[2] M. Uesaka,[1] H. Kiriyama,[3] and Y. Fukuda[3, b)]

[1)]*Nuclear Professional School, School of Engineering, The University of Tokyo, 2-22 Shirakata Shirane, Tokai, Naka, Ibaraki 319-1188, Japan*

[2)]*Graduate School of Maritime Sciences, Kobe University, 5-1-1 Fukaeminamimachi, Higashinada, Kobe, Hyogo 658-0022, Japan*

[3)]*Kansai Photon Science Institute (KPSI), National Institutes for Quantum Science and Technology (QST), 8-1-7 Umemidai, Kizugawa, Kyoto 619-0215, Japan*

[4)]*Graduate School of Energy Science, Kyoto University, Gokasho, Uji, Kyoto 611-0011, Japan*

[5)]*F-lab, Nagoya University, Furo-cho, Chikusa-ku, Nagoya, Aichi 464-8602, Japan*

[6)]*National Institute of Radiological Sciences (NIRS), National Institutes for Quantum Science and Technology (QST), 4-9-1 Anagawa, Chiba 263-8555, Japan*

(Dated: 8 February 2022)

Multi-MeV high-purity proton acceleration by using a hydrogen cluster target irradiated with repetitive, relativistic intensity laser pulses has been demonstrated. Statistical analysis of hundreds of data sets highlights the existence of markedly high energy protons produced from the laser-irradiated clusters with micron-scale diameters. The spatial distribution of the accelerated protons is found to be anisotropic, where the higher energy protons are preferentially accelerated along the laser propagation direction due to the relativistic effect. These features are supported by three-dimensional (3D) particle-in-cell (PIC) simulations, which show that directional, higher energy protons are generated via the anisotropic ambipolar expansion of the micron-scale clusters. The number of protons accelerating along the laser propagation direction is found to be as high as $1.6\pm0.3 \times 10^9$ /MeV/sr/shot with an energy of 2.8 ± 1.9 MeV, indicating that laser-driven proton acceleration using the micron-scale hydrogen clusters is promising as a compact, repetitive, multi-MeV high-purity proton source for various applications.

The recent advancements in both laser[1] and target fabrication techniques[2] have led to enhancement of the laser-driven ion acceleration energies to close to 100 MeV/u[3–5]. The unique characteristics of ultrashort pulses and point sources possessed by laser-accelerated ions have potential applications for various research fields, such as proton radiography[6,7], fast ignition[8,9], nuclear science[10], heavy particle radiotherapy[11] and radiation-induced processes in matter[12,13]. In laser-driven ion acceleration experiments, thin films with thicknesses from nanometers to micrometers have been widely utilized as targets for laser irradiation[14,15]. However, in such experiments, regardless of the target material, not only protons, but also other ion species, such as carbon and oxygen, all of which originate from surface contaminants of thin films, are accelerated together, making the production of high-purity proton beams unrealistic.

From the viewpoint of practical applications, impurity-free multi-MeV proton beams have a great advantage. Therefore, laser acceleration of protons with various types of hydrogen targets has recently attracted much attention. For example, hydrogen droplets with diameters down to 10 μm[16,17], thin solid-hydrogen slabs[18] and ribbons[19–22] with thicknesses in the tens of μm range, and liquid cryogenic microjets[23–26] have been proposed and utilized in laser acceleration experiments. In addition, a high-density hydrogen gas jet has been utilized in laser acceleration experiments as a near critical density medium for near-infrared[27–29] and infrared[30] lasers.

Here, to increase the possibility of high-purity proton acceleration, we employ a different approach using micron-scale hydrogen clusters with a spherical shape[31,32], which is an alternative to other types of hydrogen targets that allows very efficient coupling with laser pulses compared to planer-shaped targets[33], thus exhibiting prominent linear and nonlinear dynamics and associated optical properties[34–36] even in the radiation-dominant regime[37]. Notably, unlike previous approaches with the nanometer-scale hydrogen clusters[38–42], this approach uses micron-scale hydrogen clusters, which exhibit a unique laser-cluster interaction. Satisfying certain conditions of laser properties and cluster size, the internal degree of freedom of micron-scale hydrogen clusters causing converging shock has been utilized in achieving quasimonoenergetic protons up to the sub-GeV energy range[43].

In this work, we report the experimental demonstration of laser-driven multi-MeV high-purity proton acceleration utilizing the micron-scale hydrogen clusters at a 0.1 Hz repetition rate. Due to the replenishable target and the repetition rate laser, statistical analysis of hundreds of data sets has been conducted, which highlights the existence of markedly high energy protons generated from the laser-irradiated micron-scale clusters. Three-dimensional (3D) particle-in-cell (PIC) simulations suggest that the anisotropic ambipolar expansion

[a)]Present address: Tono Geoscience Center, Japan Atomic Energy Agency, 959-31, Jorinji, Izumi-cho, Toki, Gifu 509-5102, Japan

[b)]Corresponding author. E-mail: fukuda.yuji@qst.go.jp

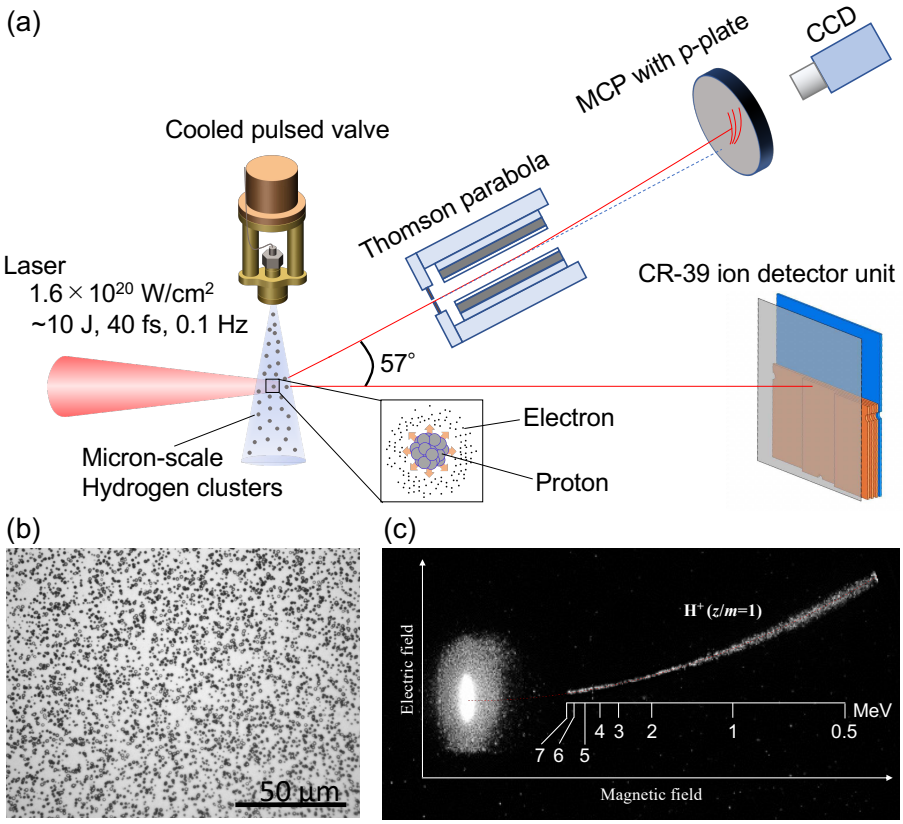

FIG. 1. **Experimental setup and proton signals.** (a) Schematic of the experimental setup for laser-driven proton acceleration. (b) Micrograph of etch pits for >0.93 MeV protons registered on the front surface of the CR-39 plate at the nozzle temperature of 25 K. (c) Single-shot proton signals detected using the real-time-type Thomson parabola at the nozzle temperature of 25 K. The vertically long elliptical bright spot is the laser focus area. The red dotted line represents the calculated ion trace with $z/m = 1$.

mechanism works for the laser-irradiated micron-scale clusters, which gives multi-MeV protons of over 10 MeV in the laser propagation direction.

The experiment was conducted using the repetitive petawatt J-KAREN-P laser facility at QST-KPSI, which is based on an OPCPA/Ti:sapphire hybrid architecture[44,45]. A schematic of the experimental setup is shown in Fig. 1(a). The laser delivers 37±5 fs duration (FWHM) pulses of 9 J energy to the target at a 0.1 Hz repetition rate with a contrast ratio of 10^{-11}. The laser pulse was focused to a 20 μm diameter ($1/e^2$) spot using an F/10 off-axis parabolic mirror, which yielded a peak intensity of 1.6×10^{20} W/cm^2 under vacuum. High energy ions were generated when the laser pulses were focused into the center of the cluster gas flow at a distance of 15-20 mm from the nozzle outlet. The pulsed valve opening timing was synchronized to the laser pulse to optimize the laser-cluster interactions. To characterize accelerated ion energies, two different types of ion detectors, an integration-type CR-39 plate installed along the laser propagation direction[46] and a real-time-type Thomson parabola[47] installed at an angle of 57 degrees with respect to the laser propagation direction, were employed.

In the present experiment, the micron-scale hydrogen clusters were produced via spallation of the liquid or supercritical fluid phase of hydrogen, namely, by expanding supercooled (25 or 50 K), high-pressure(6 MPa) molecular hydrogen gas into vacuum through a conical nozzle with an orifice diameter of 250 μm and a conical angle of 40° connected to an Even-Lavie pulsed valve (EL-5-H-2019, Atad Digital Technology Trading and Marketing Ltd.)[32,48]. To cool the gas temperature, the pulsed valve was attached to a compact closed-cycle helium refrigerator (RDK-408E2, Sumitomo Heavy Industries, Ltd.). The temperature of the pulsed valve and the nozzle was monitored using a silicon diode temperature sensor (DT-670C-SD, Lake Shore Cryotronics, Inc.) and stabilized using two high-power thick-film resisters (RTO 50, Vishay Intertechnology, Inc.) connected to a temperature controller (Model 335, Lake Shore Cryotronics, Inc.).

The size distribution of the micron-scale hydrogen clusters was evaluated by Mie scattering measurements[31,32]. With a nozzle temperature of 50 K, the size distribution was mostly peaked at 0.3 μm in diameter, while with a nozzle temperature of 25 K, in addition to the 0.3 μm clusters, micron-scale hydrogen clusters were effectively generated, and the size distribution of the micron-scale clusters was found to be widely distributed to up to 2.3 μm in diameter[32]. Here, the

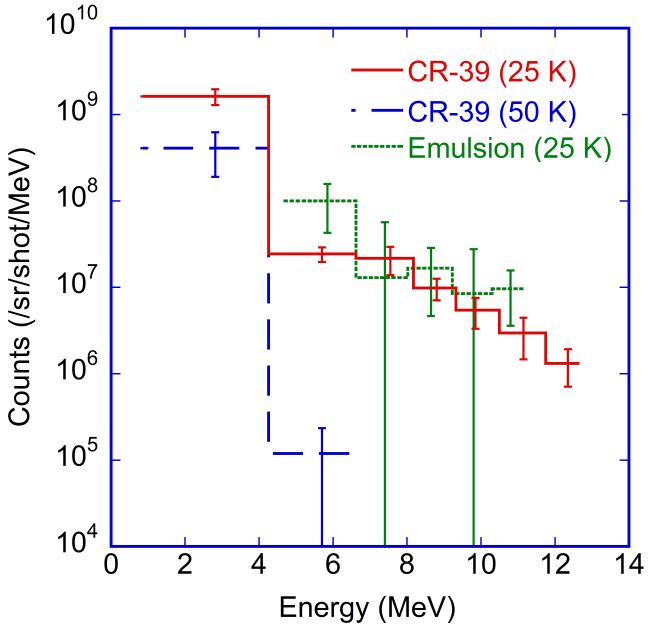

FIG. 2. **Energy spectra of laser-accelerated protons.** The energy spectra measured using the CR-39 plate with the stepwise energy filter at nozzle temperatures of 25 K (red solid line) and 50 K (blue broken line). The energy spectrum measured with the stack of nuclear emulsion films at the nozzle temperature of 25 K (green dotted line) is also shown as reference data[49]. The error bars on the y-axis represent the standard deviations of the etch pit/track counts, while those on the x- axis represent the measured energy range. These detector units were installed at a distance of 1.8 m from the laser focal point along the laser propagation direction.

mean cluster size was calculated to be 0.71±0.04 μm and 0.33±0.01 μm at nozzle temperatures of 25 and 50 K, respectively. The cluster density was estimated to be 2.0×10^9 and 4.9×10^9 clusters/cm^3 at nozzle temperatures of 25 and 50 K, respectively. The averaged intercluster distance was indirectly estimated to be 7.9 and 5.9 μm at nozzle temperatures of 25 and 50 K, respectively, from the gas phase hydrogen density obtained by optical interferometry[32].

Figure 1(b) shows a micrograph of the etch pits that appeared on the CR-39 plate. From the size of the etch pits, it is confirmed that all the accelerated ions are confirmed to belong to protons[46]. In addition, as shown in Fig. 1(c), only the single ion trace with $z/m = 1$, i.e., protons, appeared on the fluorescent imaging plate of the Thomson parabola. These results clearly demonstrate that multi-MeV impurity-free proton acceleration was achieved via the laser-irradiated micron-scale hydrogen cluster target.

Figure 2 shows the energy spectra of laser-accelerated protons measured using the 7 × 7 cm^2 integration-type detector unit with the CR-39 plate located along the laser propagation direction obtained at nozzle temperatures of 25 K and 50 K, where the ion signals were accumulated for 76 and 71 laser shots, respectively. For the case with a nozzle temperature of 25 K, the higher part of the energy spectrum obtained with the CR-39 plate is in good agreement with that obtained with the stack of nuclear emulsion films in the same series of experiments[49], which confirms that the energy spectra measurements were conducted in a technically correct manner. The maximum energy of protons accelerating along the laser propagation direction is found to be 12.4±0.6 MeV with the number of protons 1.3±0.6 × 10^6 MeV/sr/shot, while the number of protons with the lower energy of 2.8±1.9 MeV is found to be approximately 1.6±0.3 × 10^9 /MeV/sr/shot. Concerning the number of protons below 0.9 MeV detected by the CR-39 plate is estimated to be an order of magnitude larger than 10^9 /MeV/sr/shot. For the case with the nozzle temperature of 50 K, the maximum proton energy of up to 5.7±1.0 MeV is discernible.

Figures 3(a) and (b) show a series of single-shot energy spectra for 20 consecutive shots measured using the real-time-type Thomson parabola at nozzle temperatures of 25 K and 50 K, respectively. The energy spectra for 25 K have quite large fluctuations, while those for 50 K are stable. The production of lower energy protons ranging below ∼1 MeV is quite stable for both temperatures, and the number of such protons is found to be close to 10^{10} /MeV/sr/shot. Note that the number of protons below ∼1 MeV measured by the real-time-type Thomson parabola is consistent with the value estimated by the CR-39 plate within the experimental error.

Similar energy spectra data sets were obtained for 327 and 76 laser shots at nozzle temperatures of 25 K and 50 K, respectively. To understand the locality, spread, and skewness of the data sets, a box-and-whisker plot with whiskers drawn within the 1.5 interquartile range (IQR)[50] was created for the maximum energies of each data set (see Fig. 4). Here, the box is drawn from the 25th percentile (Q1) to the 75th percentile (Q3) with a horizontal line drawn in the middle to denote the median, and the cross mark represents the mean of the data

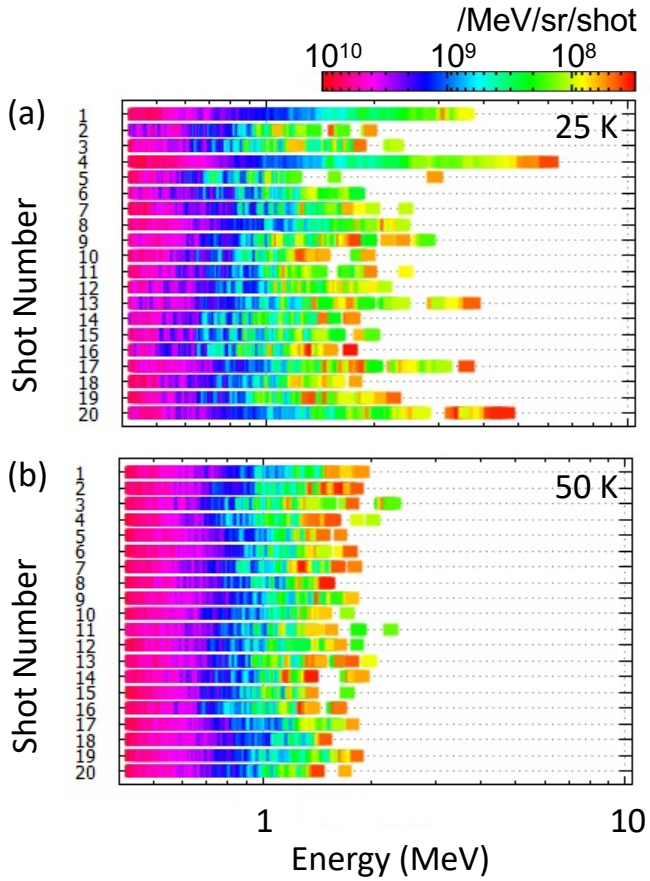

FIG. 3. **Shot-to-shot properties of laser-accelerated protons.** Series of single-shot energy spectra for 20 consecutive shots measured using the real-time-type Thomson parabola at nozzle temperatures of (a) 25 K and (b) 50 K. The color scale displays the number of ions.

set. First, both data sets are clearly far from the normal distribution, especially in the case for the nozzle temperature of 25 K, and there exists strong inhomogeneity. Second, half of the data set is concentrated between 1.2 and 2.4 MeV for the nozzle temperature of 25 K, while it is concentrated in a much narrower region between 1.3 and 1.6 MeV for the nozzle temperature of 50 K. Third, the circles plotted on the box-plot demonstrate outliers, which are defined as values greater than 1.5 IQR plus the third quartile. The number of outliers observed for the nozzle temperature of 25 K indicates the strong inhomogeneity of the data set, while the outliers are less observable for the nozzle temperature of 50 K. This result can be explained in relation to the difference in the size distributions of the clusters with respect to the nozzle temperature: For the 50 K case, only clusters with a monolithic size distribution peaking at 0.33 ± 0.01 μm exist[32], which results in Coulomb explosion of equivalent scale and gives almost the same energy spectra (see Fig. 3(b)). In contrast, for the 25 K case, clusters with a widely spread size distribution exist[32], where, in addition to the major component peaking at 0.33 ± 0.01 μm, a small number of larger sized clusters with diameters over 1 μm exist, which occasionally produce higher energy tail protons if the laser pulse hits such micron-scale clusters.

Comparing the maximum proton energies measured in the different directions at the nozzle temperature of 25 K, another interesting point is noted: The maximum proton energy of 12.4 MeV$\pm$0.6 MeV measured in the laser propagation direction is found to be much larger than the value of 7.4 MeV$\pm$0.5 MeV measured at an angle of 57 degrees with respect to the laser propagation direction, which indicates that the acceleration dynamics in the laser plasmas created via the laser-cluster interaction have inhomogeneity.

To capture the essential dynamics of acceleration, the interaction processes of a single hydrogen cluster having a diameter of 0.33, 1.2, or 2.0 μm with an intense laser pulse were investigated with the 3D PIC simulations (see Fig. 5). When the leading edge of the laser pulse reaches the cluster, the laser field expels electrons from the peripheral region of the cluster, and the expelled electrons are pushed forward along the general laser propagation direction, forming waves in the electron density due to the relativistic effect caused by the Lorenz force $v \times B$. In the case of micron-scale clusters with diameters of 1.2 and 2.0 μm, most of the electrons, 98.4 % and 95.7 %, respectively, remain unstripped inside of the clusters (see Fig. 5(a)). In this case, the ion dynamics are partially coupled to the electron dynamics, resulting in an ambipolar

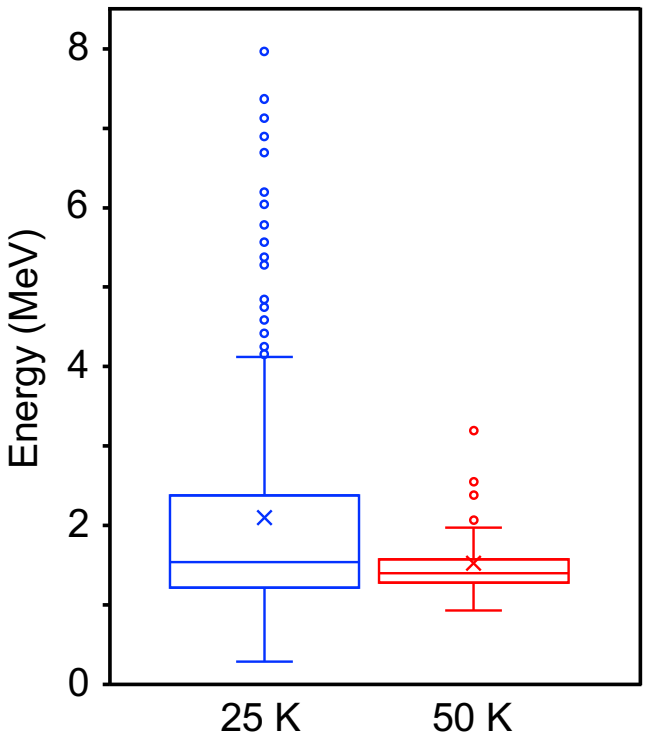

FIG. 4. **Statistical analysis highlights the existence of markedly high energy protons.** Box-and-whisker plot for the maximum energies of the each data set for nozzle temperatures of 25 K (blue) and 50 K (red). The box is drawn from the 25th percentile (Q1) to the 75th percentile (Q3), with a horizontal line drawn in the middle to denote the median, and the cross mark represents the mean of the data set. The circles demonstrate outliers, which are defined as values greater than 1.5 IQR plus the third quartile.

expansion, where the peripheral region of the cluster undergoes Coulomb explosion that produces the largest energy ions, while the core region of the cluster undergoes a hydrodynamic expansion that produces the smaller energy ions[35,51,52]. Here, in the case of micron-scale clusters, since the expelled electrons moving in the laser propagation direction drag protons located at the expanding front, the resultant ambipolar expansion becomes anisotropic, as shown in Fig. 5(b), which supports the experimental observation.

Another characteristic of ambipolar expansion is that the maximum ion energy does not sensitively depend on the size of clusters since only the peripheral region, the depth of which is determined by the electron skin depth, of the cluster undergoes Coulomb explosion. This trend is seen in Fig. 5(c), which shows the maximum energies for the hydrogen clusters with diameters of 1.2 and 2.0 μm are almost the same, 12.8 and 13.5 MeV, respectively. Note that according to the Coulomb explosion model, the maximum energies for the hydrogen clusters with diameters of 1.2 and 2.0 μm are quite differently calculated as 100 and 276 MeV, respectively. Therefore, the anisotropic ambipolar expansion of clusters with diameters of 1.2 and 2.0 μm corresponds well to the experimental observation of a maximum proton energy of 12.4$\pm$0.6 MeV measured in the laser propagation direction with a nozzle temperature of 25 K including micron-scale hydrogen clusters.

In contrast, in the case of the cluster with a diameter of 0.33 μm, only 0.57 % of the electrons remain unstripped when the peak of the laser pulse reaches the cluster center. Therefore, the ion dynamics are practically decoupled from the electron dynamics, and the whole cluster is strongly positively charged, resulting in Coulomb explosion. In the case of Coulomb explosion[35], the maximum energy for hydrogen clusters with diameters of 0.33 μm is calculated as 7.5 MeV. In the present 3D PIC simulation, this results in a maximum proton energy of 5.8 MeV, as shown in Fig. 5(c), which also corresponds well to the experimental observation of a maximum proton energy of 5.7$\pm$1.0 MeV measured in the laser propagation direction at a nozzle temperature of 50 K (see Fig. 2).

To conclude, multi-MeV protons are accelerated at a 0.1 Hz repetition rate via laser irradiation of micron-scale hydrogen cluster targets at a laser intensity of 1.6×10^{20} W/cm^2. According to the statistical data analysis, markedly high-energy protons are generated from the micron-scale hydrogen clusters. The anisotropic spatial distribution of the accelerated protons, in which the higher energy protons are preferentially accelerated along the laser propagation direction, can be attributed to the anisotropic ambipolar expansion of the micron-scale hydrogen clusters. The 3D PIC simulations with parameters that match the experimental conditions support these experimental observations. The method can offer a com-

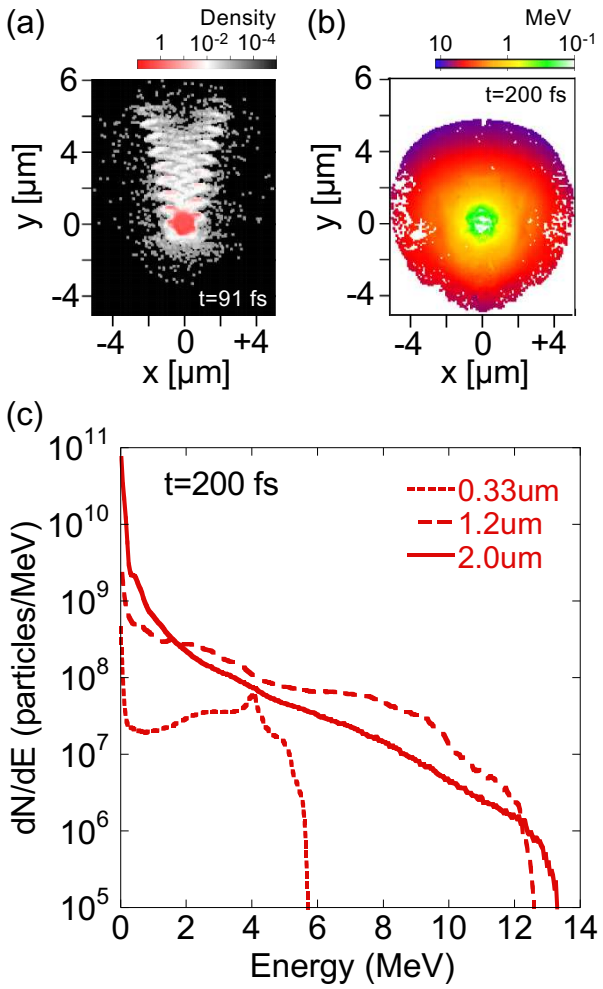

FIG. 5. **Anisotropic ambipolar expansion of the micron-scale hydrogen clusters.** 2D images of (a) electron density and (b) ion kinetic energy distributions in the x-y plane for a hydrogen cluster with a diameter of 1.2 μm at different times. The density is normalized by the initial charge density of the cluster electrons and displayed on a log scale. (c) Proton energy spectra for clusters with diameters of 0.33, 1.2, and 2.0 μm. The proton number is evaluated using a real value by multiplying the particle weight by the PIC particle number.

pact, high-purity proton source for various practical applications because such a proton source is inherently impurity-free, highly reproducible, debris-free, and robust.

Method

Integration-type ion detector unit with the CR-39 plate. The energies of protons accelerated along the laser propagation direction were measured by using an integration-type detector unit[46] composed of a 7×7 cm^2 CR-39 (HAZLAS (TD-1), Fukuvi Chemical Industry) plate, the lower half of which was covered by three stepwise layers of radiochromic films (XR-RV3, Gafchromic) that work as an energy filter. The detector unit, covered by 13 μm thick aluminium foil, was installed in the vacuum chamber at a distance of 1.8 m from the focal point along the laser propagation axis. After the measurements, the CR-39 plate was chemically etched in stirred 6 M-KOH solution kept at 70°C for 2 hours. By counting the number of etch pits on the CR-39 plate using a fast automated digital imaging optical microscope (HSP-1000, Seiko Precision Inc.), the energy spectrum was reconstructed by plotting the number of etch pits in each energy region defined by the stepwise energy moderator, the details of which are described in ref. [46].

Real-time-type Thomson parabola ion detector. To understand the shot-to-shot properties of the accelerated proton beam, the accelerated proton energies were measured on a single shot basis using a real-time-type Thomson parabola spectrometer[47], installed at an angle of 57 degrees with respect to the laser propagation direction. In the real-time Thomson parabola, after passing through a 600 μm-diameter entrance pinhole located 1.4 m from the laser focal point, ions travel through 100-mm homogeneous electric (400 V/mm) and magnetic (1.6 T) fields, where ions are differentiated by the mass-to-charge ratio and the energy, and are detected by a chevron microchannel plate (MCP) with a diameter of 75

mm equipped with a fluorescent (P20) imaging plate (3075PS, BURLE), where ions with the same charge-to-mass ratio trace the same parabola in the detector plane. The 2D image of the ion trace that appeared on the fluorescent imaging plate was monitored by the a 10-bit CMOS camera (DMK33GP1300, Imaging Source). From the brightness of the fluorescent imaging plate, the number of protons (/MeV/sr/shot) was roughly estimated using a calibration factor of the order of 10 counts/proton, obtained in a separate calibration experiment, where the solid angle is defined by the pinhole located at the entrance of the Thomson parabola spectrometer.

Particle-in-cell (PIC) simulations. The 3D PIC simulations were conducted by employing the EPIC3D code[53]. A single hydrogen cluster with an electron density of 4.6×10^{22} cm^{-3}(= 26.8 n_c) was placed at the center of a system with a size of $L_x = L_z = 10.24$ μm and $L_y = 20.48$ μm; here, n_c is the critical density of plasma corresponding to the laser wavelength $\lambda = 810$ nm. The cluster was surrounded by ambient hydrogen gas with an electron density of 4.0×10^{19} cm^{-3} (= 0.024 n_c). A grid size of 80 nm was employed to resolve the cluster explosion dynamics. A laser pulse linearly polarized in the x direction with a wavelength $\lambda = 810$ nm and a pulse duration of 33 fs (FWHM) was propagated in the $+y$ direction. The peak intensity of the laser pulse was set to 1.2×10^{20} W/cm^2 (corresponding to the normalized amplitude of a laser $a_0 = 7.8$, where $a_0 = eE/m_e c\omega$). The transparent boundary condition was used in the y direction, while the periodic boundary condition was used in the x and z directions. A fully ionized hydrogen plasma was employed as an initial condition.

References

[1] C. N. Danson et al. Petawatt and exawatt class lasers worldwide. *High Power Laser Sci. Eng.*, 7:e54, 2019.

[2] I. Prencipe et al. Targets for high repetition rate laser facilities: needs, challenges and perspectives. *High Power Laser Sci. Eng.*, 5:e17, 2017.

[3] F. Wagner et al. Maximum proton energy above 85 MeV from the relativistic interaction of laser pulses with micrometer thick CH_2 targets. *Phys. Rev. Lett.*, 116:205002, 2016.

[4] I. J. Kim et al. Radiation pressure acceleration of protons to 93 mev with circularly polarized petawatt laser pulses. *Phys. Plasmas*, 23:070701, 2016.

[5] A. Higginson et al. Near-100 mev protons via a laser-driven transparency-enhanced hybrid acceleration scheme. *Nat. Commun.*, 9:724, 2018.

[6] M. Borghesi et al. Electric field detection in laser-plasma interaction experiments via the proton imaging technique. *Phys. Plasmas*, 9:2214–2220, 2002.

[7] L. Romagnani et al. Dynamics of electric fields driving the laser acceleration of multi-mev protons. *Phys. Rev. Lett.*, page 195001, 2005.

[8] M. Roth et al. Fast ignition by intense laser-accelerated proton beams. *Phys. Rev. Lett.*, 86:436–439, 2001.

[9] J.C. Fernández et al. Fast ignition with laser-driven proton and ion beams. *Nucl. Fusion*, 54:054006, 2014.

[10] K. W. D. Ledingham, R. P. Singhal, P. McKenna, and I. Spencer. Laser induced nuclear physics and applications. *Nucl. Phys. A*, 752:633c, 2005.

[11] S.V. Bulanov and V.S. Khoroshkov. Feasibility of using laser ion accelerators in proton therapy. *Plasma Phys. Rep.*, 28:453–456, 2002.

[12] T. G. White et al. Observation of inhibited electron-ion coupling in strongly heated graphite. *Sci. Rep.*, 2:889, 2012.

[13] B. Dromey et al. Picosecond metrology of laser-driven proton bursts. *Nat. Commun.*, 7:10642, 2016.

[14] H. Daido, M. Nishiuchi, and A. S. Pirozhkov. Review of laser-driven ion sources and their applications. *Rep. Prog. Phys.*, 75:056401, 2012.

[15] A. Macchi, M. Borghesi, and M. Passoni. Ion acceleration by superintense laser-plasma interaction. *Rev. Mod. Phys.*, 85:751–793, 2013.

[16] R. A. Costa Fraga et al. Compact cryogenic source of periodic hydrogen and argon droplet beams for relativistic laser-plasma generation. *Rev. Sci. Instrum.*, 83:025102, 2012.

[17] J. Polz et al. Efficient laser-driven proton acceleration from a cryogenic solid hydrogen target. *Sci. Rep.*, 9:16534, 2019.

[18] S. Bedacht. Laser-driven ion acceleration with cryogenic hydrogen targets. *GSI Scientific Report 2013*, PNI-PP-11:192, 2014.

[19] S. Garcia et al. Continuous production of a thin ribbon of solid hydrogen. *Laser Part. Beams*, 32:569, 2014.

[20] D. Margarone et al. Proton acceleration driven by a nanosecond laser from a cryogenic thin solid-hydrogen ribbon. *Phys. Rev. X*, 6:041030, 2016.

[21] S. D. Kraft et al. First demonstration of multi-mev proton acceleration from a cryogenic hydrogen ribbon target. *Plasma Phys. Control. Fusion*, 60:044010, 2018.

[22] A. Girard et al. Cryogenic hydrogen targets for proton beam generation with ultra-intense lasers. *IOP Conf. Series: Materials Science and Engineering*, 502:012160, 2019.

[23] J. B. Kim et al. Development of a cryogenic hydrogen microjet for high-intensity, high- repetition rate experiments. *Rev. Sci. Instrum.*, 87:11E328, 2016.

[24] M. Gauthier et al. High-intensity laser-accelerated ion beam produced from cryogenic micro-jet target. *Rev. Sci. Instrum.*, 87:11D827, 2016.

[25] M. Gauthier et al. High repetition rate, multi-mev proton source from cryogenic hydrogen jets. *Appl. Phys. Lett.*, 111:114102, 2017.

[26] L. Obst et al. Efficient laser-driven proton acceleration from cylindrical and planar cryogenic hydrogen jets. *Sci. Rep.*, 7:10248, 2017.

[27] F. Sylla et al. Development and characterization of very dense submillimetric gas jets for laser-plasma interaction. *Rev. Sci. Instrum.*, 83:033507, 2012.

[28] S. N. Chen et al. Collimated protons accelerated from an overdense gas jet irradiated by a 1 m wavelength high-intensity short-pulse laser. *Sci. Rep.*, 7:13505, 2017.

[29] P. K. Singh et al. Electrostatic shock acceleration of ions in near-critical-density plasma driven by a femtosecond petawatt laser. *Sci. Rep.*, 10:18452, 2020.

[30] D. Haberberger et al. Collisionless shocks in laser-produced plasma generate monoenergetic high-energy proton beams. *Nat. Phys.*, 8:95, 2012.

[31] S. Jinno et al. Characterization of micron-size hydrogen clusters using mie scattering. *Opt. Express*, 25:18775, 2017.

[32] S. Jinno et al. Micron-size hydrogen cluster target for laser-driven proton acceleration. *Plasama Phys. Control. Fusion*, 60:044021, 2018.

[33] T. Ditmire et al. High intensity laser absorption by gases of atomic clusters. *Phys. Rev. Lett.*, 78:3121, 1997.

[34] T. Tajima, Y. Kishimoto, and M. C. Downer. Optical properties of cluster plasma. *Phys. Plasmas*, 6:3759, 1999.

[35] Y. Kishimoto et al. High energy ions and nuclear fusion in laser-cluster interaction. *Phys. Plasmas*, 9:589, 2002.

[36] Th. Fennel et al. Laser-driven nonlinear cluster dynamics. *Rev. Mod. Phys.*, 82:1973, 2010.

[37] N. Iwata et al. Effects of radiation reaction in the interaction between cluster media and high intensity lasers in the radiation dominant regime. *Phys. Plasmas*, 23:063115, 2016.

[38] R. A. Smith et al. Characterization of a cryogenically cooled high-pressure gas jet for laser/cluster interaction experiments. *Rev. Sci. Instrum.*, 69:3798, 1998.

[39] S. Sakabe et al. Generation of high-energy protons from the coulomb explosion of hydrogen clusters by intense femtosecond laser pulses. *Phys. Rev. A*, 69:023203, 2004.

[40] D. R. Symes et al. Anisotropic explosions of hydrogen clusters under intense femtosecond laser irradiation. *Phys. Rev. Lett.*, 98:123401, 2007.

[41] S. Grieser et al. Nm-sized cryogenic hydrogen clusters for a laser-driven proton source. *Rev. Sci. Instrum.*, 90:043301, 2019.

[42] B. Aurand et al. Study of the parameter dependence of laser-accelerated protons from a hydrogen cluster source. *New J. Phys.*, 2:033025, 2020.

[43] R. Matsui, Y. Fukuda, and Y. Kishimoto. Quasimonoenergetic proton bunch acceleration driven by hemispherically converging collisionless shock in a hydrogen cluster coupled with relativistically induced transparency. *Phys. Rev. Lett.*, 122:014804, 2019.

[44]H. Kiriyama et al. High-contrast high-intensity repetitive petawatt laser. *Opt. Lett.*, 43:2595, 2018.
[45]A. S. Pirozhkov et al. Approaching the diffraction-limited, bandwidth-limited petawatt. *Opt. Express*, 25:20486, 2017.
[46]M. Kanasaki et al. Correction method for the energy spectrum of laser-accelerated protons measured by cr-39 track detectors with stepwise energy filters. *High Energy Density Phys.*, 37:100852, 2020.
[47]Y. Kuramitsu et al. Robustness of large-area suspended graphene under interaction with intense laser. *Sci. Rep.*, accepted.
[48]U. Even. The even-lavie valve as a source for high intensity supersonic beam. *EPJ Tech. Instrum.*, 2:17, 2015.
[49]T. Asai et al. Application of nuclear emulsions for the identi- fication of multi-mev protons in laser ion acceleration experiments. *High Energy Density Phys.*, 32:44, 2019.
[50]J. W. Tukey. *Exploratory Data Analysis*. Addison-Wesley, 1977.
[51]Y. Fukuda et al. Structure and dynamics of cluster plasmas created by ultrashort intense laser fields. *Phys. Rev. A*, 73:031201R, 2006.
[52]R. Matsui, Y. Fukuda, and Y. Kishimoto. Dynamics of the boundary layer created by the explosion of a dense object in an ambient dilute gas triggered by a high power laser. *Phys. Rev. E*, 100:013203, 2019.
[53]Y. Kishimoto et al. A paradigm of kinetic simulation including atomic and relaxation processes: a sudden event in a lightning process. *J. Plasma Phys.*, 72:971, 2006.

Acknowledgements

The authors express our thanks to the J-KAREN-P laser facility staff for their kind support throughout the experiments. This work was supported by a JSPS KAKENHI Grant (No. 19H00668) and a QST President's Strategic Grant (Creative Research).

Author contributions

S.J., M.K., T.A., A.S.P., K.O., A.S., Y.M., N.N., M.K., H.K., and Y.F. carried out the experiment with J-KAREN-P. T.A., N.K., and K.M. conducted ion detection with the nuclear emulsion film and analyzed the data. M.K., T.A., and T.Y. conducted ion detection with the CR-39 plate and analyzed the data. S.J. conducted ion detection with the Thomson parabola and analyzed the data. S.K. supported the calibration experiments of the ion detectors with HIMAC. R.M., and Y.K. conducted the 3D PIC simulations and analyzed the data. Scientific discussions were provided by M.U.. The paper was written by S.J. and Y.F..